LA-UR 91-1158

LA-UR--91-1158

TI91 011394

TITLE LASER-BASED DIAGNOSTICS FOR CONDENSATION IN LASER-ABLATED COPPER PLASMAS

AUTHOR(S) Andrew D. Sappey, CLS-3
Thomas K. Gamble. CLS-3

SUBMITTED TO 22nd Fluid Dynamics, Plasma Dynamics and Lasers Conference
June 24 through June 27, 1991

DISCLAIMER

MASTER

Los Alamos Los Alamos National Laboratory
Los Alamos, New Mexico 87545

AIAA 91-1460

Laser-Based Diagnostics for Condensation in Laser-Ablated Copper Plasmas

A. D. Sappey and T. K. Gamble
Los Alamos National Laboratory
Los Alamos, NM

AIAA 22nd Fluid Dynamics, Plasma Dynamics & Lasers Conference
June 24-26, 1991 / Honolulu, Hawaii

LASER-BASED DIAGNOSTICS FOR CONDENSATION IN LASER-ABLATED COPPER PLASMAS

A. D. Sappey and T. K. Gamble
Chemical and Laser Sciences Division
Los Alamos National Laboratory
Los Alamos, New Mexico 87545

Abstract

We are investigating the thermodynamic conditions under which condensation occurs in laser-ablated copper plasma plumes. The plasma is created by XeCl excimer laser ablation (308 nm, 350 mJ/pulse) at power densities from 500-1000 MW/cm^2. The atomic vapor expands rapidly into backing pressures of helium ranging from 0-50 torr. The backing gas serves to slow the vapor before it rarefies and provides a third body to stabilize collision complexes between vapor atoms to produce small cluster species. The formation of these small clusters is indicative of the onset of condensation, a process which, under the proper conditions, eventually forms macroscopic particulate in the plume. We use laser-induced fluorescence (LIF) to probe both atomic copper and the copper dimer molecule, Cu_2. Velocities of atomic Cu have been obtained by a time-of-flight method under varying conditions of backing gas pressure. At low pressure (10 mtorr), the atomic Cu velocity peaks at approximately 2 × 10^6 cm/s. Excitation scans of the Cu_2 A - X (0,0) and (1,1) bands yield both a rotational temperature and a vibrational temperature. Direct laser beam absorption is used to determine the number density of atomic copper. Rayleigh scattering from particulate is easily observable under conditions favorable to particulate production. The Cu_2 LIF and Rayleigh-scattered signals disappear instantaneously in the absence of the ablation laser pulse indicating that the particulate is formed during a single laser shot.

Introduction

Laser ablation is a remarkably general method for producing refractory materials in the gas phase. Laser ablation sources are used in spectroscopic studies of gas-phase metal clusters.[1] Commercial applications of laser ablation include the production of thin films of materials such as superconductors and fine metallic powders.[2,3] In the case of thin film production, it is desirable to avoid gas-phase condensation of the plume species which would produce inhomogeneities in the film, while condensation is necessary for the production of fine metallic powders. In both cases, knowledge of the conditions under which condensation takes place in the plume is of paramount importance for understanding the condensation phenomenon and optimization of the process.

To date much of the present knowledge regarding condensation in laser-ablated plasmas is the result of work performed by Smalley and coworkers who developed a laser ablation source for the production and spectroscopic characterization of small metal clusters, M_n (M_n, n typically less than 200).[4] In this source, a laser beam is focused on to a metal rod that is rotating inside a holder. The holder is attached to the end of a pulsed molecular beam valve. As the ablation laser is fired, the valve is opened allowing a high-density buffer gas pulse to entrain atomic material from the rod. The buffer gas and atomic species travel down a narrow channel (typically 1-3 mm in diameter). The buffer gas cools the ablated material and provides a third body to stabilize collision complexes between atomic and small molecular species to foster growth of the cluster species. The clusters expand into a vacuum at the end of the channel, which brings growth to an abrupt halt, and the resulting distribution of clusters may be analyzed by mass or optical spectrometric techniques. The distribution of clusters is found to be remarkably sensitive to both the pressure of the buffer gas pulse and the length of the channel. Higher backing pressures and longer channels foster the growth of larger clusters.[4]

Unfortunately, condensation in the Smalley source occurs inside the channel in a region that is not easily accessed for diagnostic purposes

making the study of such processes all but impossible. Variations of this source have been developed, but all share the same drawback.[5] Froben et al. claim to have developed a cluster source that has no channel.[6] That is, the pulse from the supersonic valve expands freely to entrain the metal vapor. They offer an emission spectrum in the region of the Cu_2 A-X transition as proof that the source produces clusters. However, we can assign every feature in their spectrum to Cu^*. This certainly casts doubt on their conclusion.

Lyman has used laser ablation of various target materials directly into a static background gas to produce macroscopic particulate.[3] Particulate is generally formed only with backing gas pressures above 1-5 torr. This is because at lower pressures, the atomic velocity is so high that the plume rarefies before a substantial number of collisions between plume species can occur. The background gas serves to slow and contain the atoms in a small enough volume that collisions between target material atoms can occur. In addition, the background gas provides a third body to stabilize collision complexes between atoms of the target material. This is necessary for small collision complexes, which do not have enough internal degrees of freedom to dissipate the binding energy of the new atom. The geometry of this source is such that diagnostics are easily implemented. However, no *in situ* diagnostics were performed in the previous studies to determine if the particulate is formed during a single shot or grows over a period of many hundreds of shots. We have adopted this experimental geometry and instituted *in situ* laser-based diagnostics to answer this question and to determine the thermodynamic conditions under which single shot particle production may occur.

Experimental

The experimental configuration is displayed in Fig. 1. Briefly, a 308-nm excimer laser beam (300 mJ, 15 ns) is focused by a 25-cm-focal length lens onto a rotating copper target at normal incidence. The base pressure of the test chamber is 10 mtorr and the pressure can be increased from this value to approximately 800 torr with He buffer gas. During each experiment, a slow flow of helium is maintained to minimize the build-up of background atomic Cu and particulate. The spot size at the target is approximately 0.1 cm × 0.2 cm. Copper is chosen as the target material for these studies because the spectroscopy of atomic Cu, Cu_2, and Cu_3 is relatively well understood. At a variable time delay after the ablation laser pulse, an excimer pumped dye laser is fired. For Cu atom detection, the fundamental beam at ~650 nm is frequency doubled in a KDP crystal to produce radiation in the vicinity of 325 nm. This beam passes through the apparatus parallel to the copper target and perpendicular to the ablation laser beam. Fluorescence is collected along the third axis, which is perpendicular to both the ablation laser and the probe laser by a single 8.5-cm focal length, 5-cm-diameter lens and focused on to the entrance slit of a 0.22-m monochromator. The slits of the monochromator are typically 0.1 mm wide and the height is approximately 2 mm giving a spectral resolution of 0.37 nm. The distance from the target to the probe laser beam and detection system is variable so that the plume species can be probed as a function of distance from the target as well as delay time. This allows us to determine time-of-flight profiles and velocities for all species that can be detected by LIF.

For absolute calibration of the LIF signals, direct absorption experiments are performed. In these experiments, the probe laser beam exiting the chamber impinges on a fluorescent card. The intensity of this fluorescence is monitored by a photomultiplier equipped with a neutral density filter. An absorption experiment then consists of scanning the dye laser frequency over a Cu atomic transition and observing the decrease in transmitted laser intensity. With knowledge of the dominant broadening mechanism and the degree of laser saturation, one can calculate an effective cross section and therefore a Cu number density.

The Cu_2 molecule has also been detected by LIF via the A - X (0,0) transition. To our knowledge, this is the first observation of Cu_2 produced in our experimental configuration. It has been produced previously in the Smalley source[4] and in sputtering sources.[7] The bandhead of this transition occurs at ~490.27 nm. We typically detect fluorescence on the (0,1) band at 496.7 nm to avoid contamination of the fluorescence signal by

Rayleigh scattering from the particulate. This electronic system has been studied by a number of groups, but most recently by Page et al.[7] The spectroscopic constants have been determined accurately so that spectral simulations of the (0,0) band can be computed at various temperatures and compared to experimental spectra to determine rotational and vibrational temperatures. Time-of-flight profiles can be obtained for Cu_2 in the same manner as described above for Cu.

In addition, we observe a strong Rayleigh scattered signal from the particulate at 90° to the probe beam using the monochromator/phototube as the detector. This signal comprises an unwanted interference when attempting to detect resonance fluorescence, but it is extremely useful for determining where particulate is formed in the plume. Typically, we use LIF detection schemes, which observe fluorescence transitions to levels other than the ground state to avoid this problem. Contamination of the Rayleigh scattered signal by LIF is avoided by performing the scattering experiments off of atomic or molecular resonances.

Results and Discussion

Cu Atom LIF and Absorption Diagnostics

I. Cu Atom Laser-Induced Fluorescence

Figure 2 displays an excitation scan of the $^2P_j < {}^2S$ transitions in copper atom as well as an abridged Cu energy level diagram as an inset. We excite from the ground state to the two spin-orbit levels of the ^2P state at the energies (wavelengths), 30535.302 cm^{-1} (324.754 nm) and 30783.686 cm^{-1} (327.396 nm), respectively. For this scan, fluorescence is detected at 578.4 nm to the ^2D level. The fact that we observe both ^2P_j components in the excitation scan, even though fluorescence is detected from only the lower energy ^2P_j component, is indicative that energy transfer occurs in the ^2P_j manifold on a time scale competitive with the fluorescence lifetime (~10 ns) under these experimental conditions (5-torr He background gas). This is not particularly surprising since the separation between the ^2P_j components is only ~200 cm^{-1}.

Figure 3 shows a dispersed fluorescence scan obtained by exciting the ^2P_j spin-orbit level of Cu atom at 324.754 nm. Fluorescence bands are observed at 324.8, 327.4, 510.7, 570.2, and 578.4 nm. If energy transfer between the spin-orbit levels of the ^2P_j did not occur, one would expect fluorescence at 324.8, 510.7, and 570.2 nm only. Strong resonance fluorescence is observed; however, to avoid possible contamination of the LIF signal by Rayleigh scattering from particulate, we typically observe fluorescence to the ^2D spin orbit levels. It should be noted that the ^2P and ^2D levels are the lasing levels of the copper vapor laser. In fact, under some circumstances, we observe stimulated emission (bi-directional lasing action) on the 510.7-nm transition, which is easily visible by eye.

II. Cu Number Density from Absorption Measurements

In order to quantify the number density of Cu under various backing pressure conditions, we have performed direct laser beam absorption experiments. Equation (1) gives a general expression for the transmitted intensity in an absorption experiment where i denotes the lower energy level and k the excited level; $\alpha_{ik}(\nu)$ is the frequency dependent absorption coefficient.[8]

$$dI = -\iint \alpha_{ik}(\nu)\, I(\nu)\, d\nu\, dz$$
$$\alpha_{ik}(\nu) = \alpha_0\, g(\nu - \nu_0) \qquad (1)$$

For situations in which the linewidth of the laser is less than that of the absorbing transition, I(ν) may not be taken out of the integral. In our experiment, the width of the absorption lines are typically 1 cm^{-1}, while the bandwidth of the frequency-doubled probe laser is 0.1-0.2 cm^{-1}. Therefore, I(ν) may not be taken out of the integral without approximation.

The major difficulty in evaluating Eq. (1) from experimental data is in the determination of the appropriate lineshape function, $g(\nu - \nu_0)$. For situations in which only saturation broadening occurs, the expected lineshape is Lorentzian,

while for Doppler broadening the expected lineshape is Gaussian.[8] However, both broadening mechanisms are operational in our experimental data as shown below.

The saturation parameter is defined as the ratio of the induced transition rate to the spontaneous transition rate:

$$S = B_{21} I / (A_{21} + Q_{21}) \quad . \qquad (2)$$

In Eq. (2), B is the Einstein coefficient for stimulated emission, I is the laser intensity, A is the Einstein coefficient for spontaneous emission, and Q is the quenching rate for the excited state. Unfortunately, Q is not known for Cu atom in the ^2P state, but it should be small, at least at pressures below 5 torr. We assume here that it is zero. For our typical laser conditions (10 μJ in a 0.01-cm^2 spot, 15-ns pulse; 0.1-cm^{-1} bandwidth), one calculates a saturation parameter of 11,500. That is, the laser strongly saturates the transition. For a lineshape dominated by saturation broadening, the linewidth is given by Eq. (3) where $\Delta\nu_n$ is the natural linewidth for the transition, 7.3×10^{-4} cm^{-1}.[8]

$$\Delta\nu_s = \Delta\nu_n [\sqrt{(1+S)}] \quad . \qquad (3)$$

With S equal to 11,500, the saturation broadened Lorentzian linewidth in our experiment is calculated to be 0.08 cm^{-1}. This is narrower than the laser bandwidth, and indicates that saturation broadening is not the dominant line broadening mechanism.

Saturation is not the dominant line-broadening mechanism, which is confirmed by fitting lineshape functions to the experimental data, as shown for a typical case in Fig. 4. The spectrum was obtained with 5 torr of helium backing gas at a distance of 2.5 cm from the target. In the upper panel of Fig. 4, a Gaussian lineshape is fitted to the experimental data, while the bottom panel shows a Lorentzian fit to the same data. The lineshape is clearly Gaussian and has a half-width of 1.43 cm^{-1}. The fact that the lineshape is Gaussian indicates that saturation broadening, while present, is much less important than Doppler broadening. In addition to produce a linewidth of 1.43 cm^{-1} from pure saturation broadening would require a laser energy of approximately 1.5 mJ/pulse, which is more than our laser system can produce at this wavelength. Therefore, it is clear that Doppler broadening dominates the measured linewidth.

The absorption coefficient for a saturated, Doppler broadened transition is given in terms of a constant times a lineshape function called a Voigt profile.[8] In general, the Voigt profile can not be integrated to give a closed form expression. However, for the limit in which Doppler broadening dominates, the integral can be evaluated exactly and the saturated, inhomogeneously broadened absorption coefficient becomes:

$$\alpha_s(\nu) = \{\alpha_0(\nu_0)/[\sqrt{(1+S)}]\} \exp\{-[(\nu - \nu_0)/\Delta\nu_D]^2\} \quad . \qquad (4)$$

where $\Delta\nu_D/0.6$ is the Doppler width of the transition. Two realities are evident. First, according to Eq. (4), in the limit of strong Doppler broadening and weak saturation broadening, the lineshape should be Gaussian.[8] This is the case in all of our data. Second, the absorption coefficient at line center is decreased in the saturation regime by a value of $1/\sqrt{(1+S)}$. In terms of cross section, Eq. (4) becomes:

$$\sigma_s(\nu) = \{[\sigma_0(\nu_0)[N_i - (g_i/g_k)N_k]\}/[\sqrt{(1+S)}] \exp\{-[(\nu-\nu_0)/\Delta\nu_D]^2\} \qquad (5)$$

If the excited state population is small at time zero, then Eq. (5) becomes:

$$\sigma_s(\nu) = \{[\sigma_0(\nu_0)N_i]/[\sqrt{(1+S)}]\} \exp\{-[(\nu - \nu_0)/\Delta\nu_D]^2\} \quad . \qquad (6)$$

Inserting Eq. (6) into Eq. (1) for $\alpha_s(\nu)$ and integrating over z, one obtains:

$$dI = -N\sigma_0(\nu_0)\, z/[\sqrt{(1+S)}] \int \exp\{-[(\nu - \nu_0)/\Delta\nu_D]^2\}\, I(\nu)\, d\nu \quad . \qquad (7)$$

Since the laser linewidth, $\Delta\nu_l$, is about a factor of ten less than the Gaussian linewidth, a reasonable approximation is to assume that the laser is a delta function in frequency space, $I(\nu) = I\,\delta(\nu - \nu_0)$, and evaluate the integral at ν_0. One is left with the following:

$$dI/I = -N_i\sigma_0(\nu_0)z/[\sqrt{(1+S)}] \quad . \qquad (8)$$

We analyze the data by fitting each spectrum to a Gaussian lineshape function as shown in Fig. 4.

The parameters fitted are peak position and half-width in wavenumbers, the 100% transmittance baseline, and the per cent absorption. At line center, the number density is given by Eq. (8). Integrating Eq. (8), one obtains the operative number density equation.

$$N_i = -\{\ln (I/I_0)[\sqrt{(1+S)}]\}/\sigma_0(\nu_0)z \ . \qquad (9)$$

The cross section is given in terms of the Einstein A coefficient by the following:

$$\sigma = 1.5 \times 10^{-8}(2\ p^2\ e^2/mc)\ (g_k/g_i)\ \lambda^2\ A \ . \quad (10)$$

The cross section for the $^2P_{3/2} < {}^2S_{1/2}$ transition at 325.754 nm is 5.93×10^{-16} cm^2. From this value, a calculated saturation parameter, the experimental per cent transmission, and a path length estimated from the size of the visible plume, a number density can be calculated. We must assume for the present that the Cu atoms are uniformly distributed over the path length. This can be confirmed by planar laser-induced fluorescence measurements that will commence in the near future. Typical values for Cu number densities at 5 torr are $2 - 4 \times 10^{16}$ cm^{-3}. For comparison, we remove approximately 3×10^{15} Cu atoms per laser shot. This indicates that the atoms removed must be present in a volume considerably smaller than the visible extent of the plume at 5 torr, which is approximately 8 cm^3. This is certainly possible as shown below by the Cu atom time-of-flight data.

III. Cu Atomic Velocity by Time of Flight

Figure 5 shows a series of curves whose amplitude is proportional to the number density of Cu atom at different distances from the target, as a function of delay time between the ablation laser pulse and the LIF probe laser pulse. The curves pictured in Fig. 5 were obtained under vacuum conditions (~10 mtorr). Dividing the distance travelled between two curves by the delay time difference gives a velocity. The velocities measured from Fig. 5 are approximately 2×10^6 cm/s.

In Fig. 5, the Cu atom density peaks at short delay times of 2 - 5 μs, but the signal persists at a level perhaps 20% of the peak value for times in excess of 50 μs. The data indicate that the majority of the Cu atoms are present in a spherical shell that is expanding quickly outward. This is the prediction of blast wave theory as developed by Zel' dovich and Rayzer.[9]

The situation with 5 torr of He backing gas is noticeably different. Time-of-flight curves for this condition are shown in Fig. 6. It is apparent that the backing gas slows and broadens the time-of-flight distribution considerably when compared to the low-pressure data. The average velocity of the Cu atoms 0.5 cm from the target surface is 4.4×10^5 cm/s and decreases to 1.8×10^3 cm/s 3.2 cm from the target. This trend continues when the pressure is increased to 50 torr. The velocity decreases to approximately 2×10^3 cm/s only 0.7 cm from the target.

Cu_2 LIF Detection and Temperature Measurement

Figure 7 is a fluorescence excitation scan of the Cu_2 A-X (0,0) band taken with 50 torr of background He gas. The probe laser-target distance was 0.6 cm in this case. The signal instantaneously disappears in the absence of the ablation laser pulse indicating that the Cu_2 is formed on a single shot within the plume. The A-X system of Cu_2 has been thoroughly studied previously by a number of groups, but most recently by Page, Gudeman, and Mitchell.[7] Rotational constants have been determined for both states and, therefore, rotational temperatures can be obtained by simulating the rovibronic band contours. Such a simulation of the Cu_2 A-X band (0,0) band at 300 K is given in Fig. 8. The simulation does not include features due to the (1,1) band, which are seen in the experimental spectrum of Fig. 7. The simulation does not adequately reflect the experimental spectrum, primarily because the bandhead is not intense enough relative to the rotational structure in the 491.0- to 492.0-nm region. Based on simulations at higher temperatures, we believe that this is an experimental artifact due to some combination of detection electronics saturation and non-uniform monochromator spectral response. Both problems are being remedied. However, it is apparent that the temperature in the experimental scan is relatively low, being in the neighborhood of 300 K.

In principle, the ratio of the (0,0) and (1,1) bandhead intensities can be used to calculate a vibrational temperature assuming a Boltzmann distribution in the ground-state Cu_2 vibrational distribution. This temperature is also approximately 300 K based on the spectrum of Fig. 7; however, it is subject to the same experimental biases as discussed for the rotational temperature above. The fact that these temperatures are quite low seems somewhat surprising; however, at room temperature the collision frequency for 50 torr of He is 3×10^8 s^{-1}, and it is most likely somewhat higher in our experiment. After a Cu_2 molecule is formed, it undergoes a collision approximately every 33 ns; after several such collisions it will be thermalized. Therefore, it is not surprising that we observe room temperature Cu_2 with 50 torr of background gas. In order to observe the nascent temperature, one must use lower pressures of backing gas.

Figure 9 shows time-of-flight curves for Cu_2 with 50 torr of He backing gas obtained in the same manner as those for Cu in Figs. 5 and 6. The relative signal intensities for each position are approximately correct. Two realities are noteworthy. First, the Cu_2 is moving extremely slowly under these conditions. This is not particularly surprising considering the collision frequency. Second, although there appears to be a higher number density of Cu_2 at z = 2.5 cm from the relative signal strengths, one must also consider the effect of temperature on the signal. The laser excited the bandhead in each of the three curves of Fig. 9. The bandhead in the Cu_2 A-X system occurs in the R-branch at relatively low J (J = 16). At low temperature, most of the intensity accumulates in the bandhead, while at high temperature the bandhead is diminished in intensity. Therefore, in order to make a direct comparison of relative Cu_2 number density, one must know the temperature as well as the signal strength on the bandhead.

Rayleigh Scattering from the Particulate

In addition, we have observed Rayleigh scattering from the condensate formed in the plasma plume with 50 torr of helium background gas. The signal instantaneously disappears in the absence of the ablation laser pulse indicating that the particulate is formed on a single shot within the plasma plume. The Rayleigh-scattered signal was observed to be a factor of 2 -3 stronger than the Cu_2 LIF signal when resonance fluorescence is detected. The strength of the Rayleigh signal is somewhat surprising considering the small size ($\leq$150 nm)[10] of the particles relative to the 490.3-nm pump wavelength. This signal can be used to measure the location and velocity of the particles.

Conclusions and Future Directions

We have developed diagnostics for Cu number density and velocity as well as for Cu_2 detection, velocity, and temperature in laser-ablated copper plasmas. These diagnostics allow us to measure very high Cu velocities (2×10^6 cm/s) in the absence of any added backing gas as well as the effect on velocity of a backing gas. Copper atom densities are as high as $2 - 4 \times 10^{16}$ cm^{-3} with 5 torr of He background gas assuming a uniform distribution of Cu atoms across the plume. Vibrational and rotational temperatures for Cu_2 with 50 torr of He backing gas are approximately 300 K, 0.6 cm from the target surface, but further development of the temperature diagnostic is necessary to refine the measurement. The temperature is necessary to place the Cu_2 LIF signal (number density) on a relative scale because of the effect of temperature on the intensity of the bandhead. Rayleigh scattering from the particulate is quite strong at 50 torr, and this signal can be used to measure the location and velocity of the particles. The LIF signal from Cu_2 and the Rayleigh-scattered signal from the particles instantaneously disappears in the absence of the ablation laser pulse indicating that the particles are formed on a single laser shot. Future experiments will obtain two-dimensional images of Cu atoms, Cu_2, and particulate in an attempt to correlate the disappearance of Cu atom with the appearance of Cu_2 and ultimately particulate. In addition, we intend to search for Cu_3 via LIF diagnostics.

References

1. E. A. Rohlfing and J. J. Valentini, J. Chem. Phys. **84**, 6560 (1986).

2. See for example, X. D. Wu, R. E. Muenchausen, S. Foltyn, R. C. Estler, R. C. Dye, C. Flamme, N. S. Nogar, A. R. Garcia, J. Martin, and J. Tesmer, Appl. Phys. Lett. **56**, 1481 (1990).

3. J. L. Lyman, *Synthesis of Materials with Infrared and Ultraviolet Lasers*, SPIE Proceedings # 1033 International Conference on Trends in Quantum Electronics, Central Institute of Physics, Bucharest, Romania (1988).

4. D. E. Powers, S. G. Hansen, M. E. Geusic, D. L. Michalopoulos, and R. E. Smalley, J. Chem. Phys. **78**, 2866 (1983).

5. B. H. Weiller, P. S. Bechthold, E. K. Parks, L. G. Pobo, and S. J. Riley, J. Chem. Phys. **91**, 4714 (1989).

6. F. W. Froben, J. Kolenda, and K. Moller, J. Phys. D **12**, 485 (1989).

7. R. H. Page and C. S. Gudeman, J. Chem. Phys. **94**, 39 (1991).

8. W. Demtroder, *Laser Spectroscopy: Basic Concepts and Instrumentation*, Springer Series in Chemical Physics 5, Springer-Verlag Berlin (1981).

9. Zel'dovich, Ya. B. and Rayzer, Yu. P., *Physics of Shock Waves and High Temperature Gas Dynamic Phenomena*, Moscow Nauka (1966).

10. A. D. Sappey, T. K. Gamble, P. J. Wantuck, H. H. Watanabe, and B. Benjamin, *Diagnostic Studies of Laser Ablated Iron Plasmas*, Los Alamos Unclassified Report #90-3258 (1990).

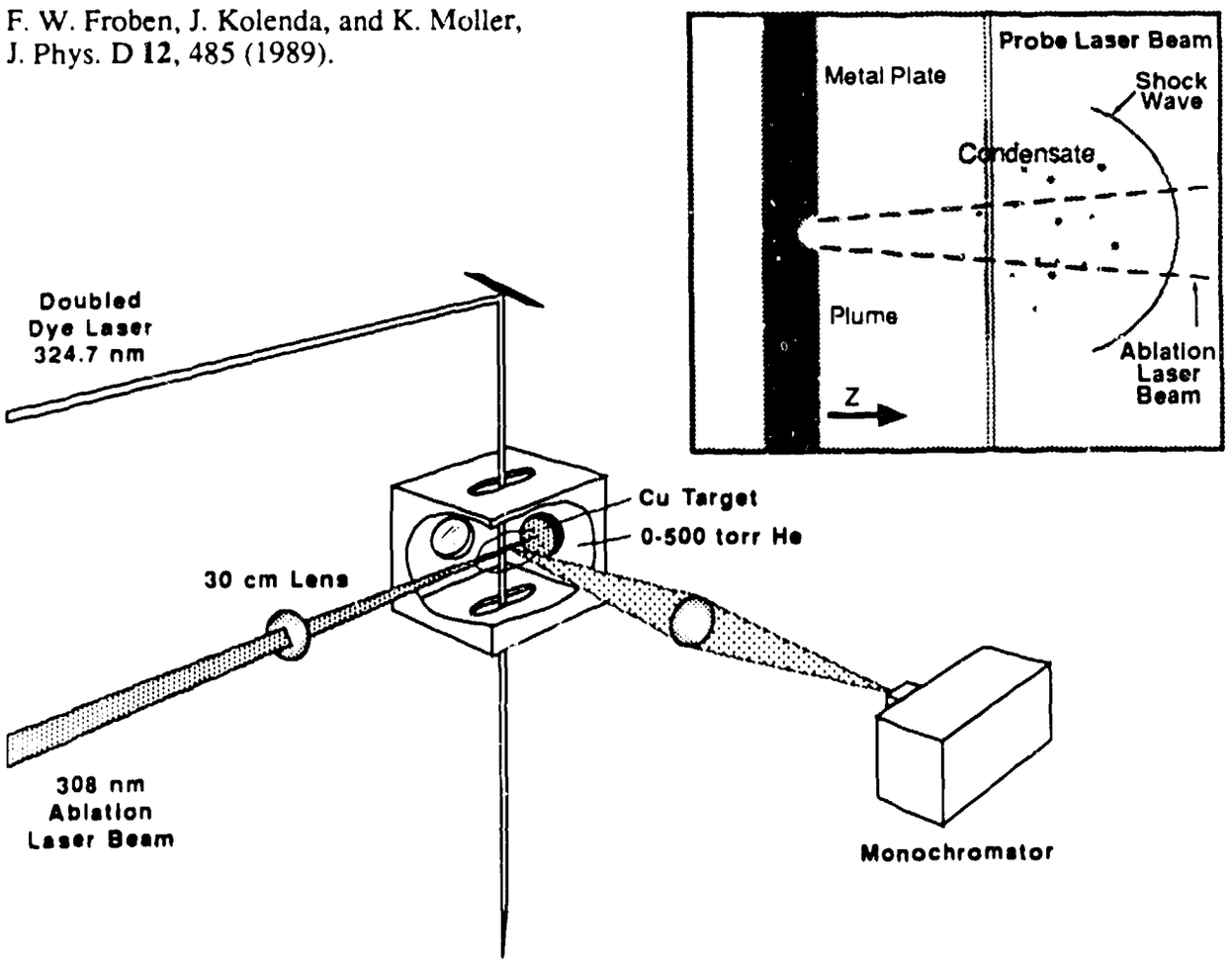

Fig. 1. Schematic diagram of Laser-Induced Fluorescence Apparatus. Inset shows details of the ablation plume and the probe laser beam.

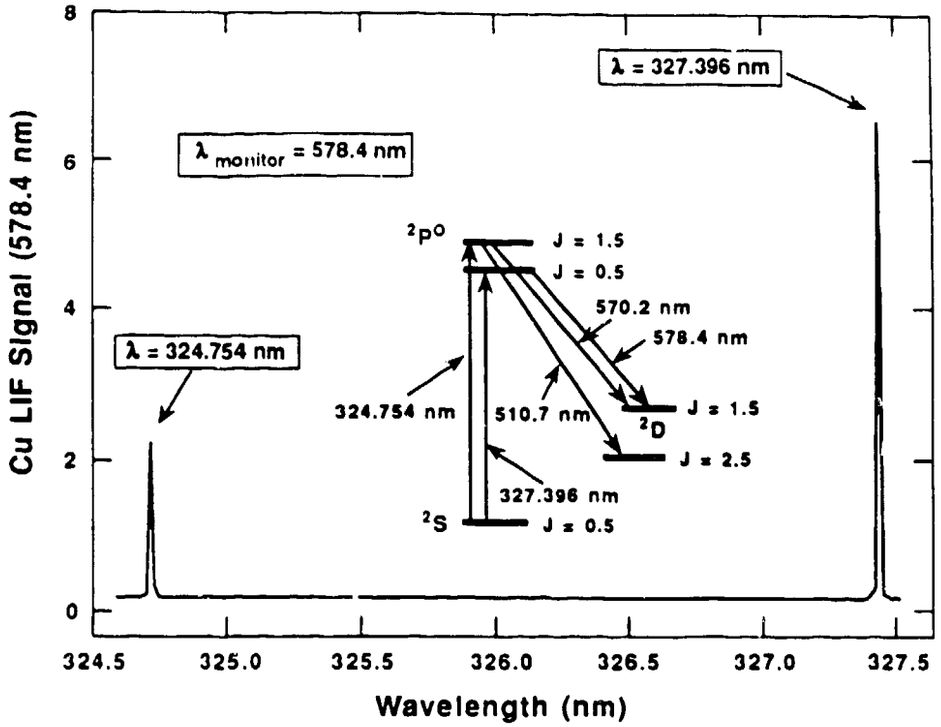

Fig. 2. Laser-induced fluorescence scan of the Cu atom $^2P^0 \leftarrow {}^2S$ transitions. Fluorescence is detected at 578.4 nm. The probe laser is located 2.5 cm from the surface and the backing gas pressure is 5 torr He. The delay between the lasers is 500 μs.

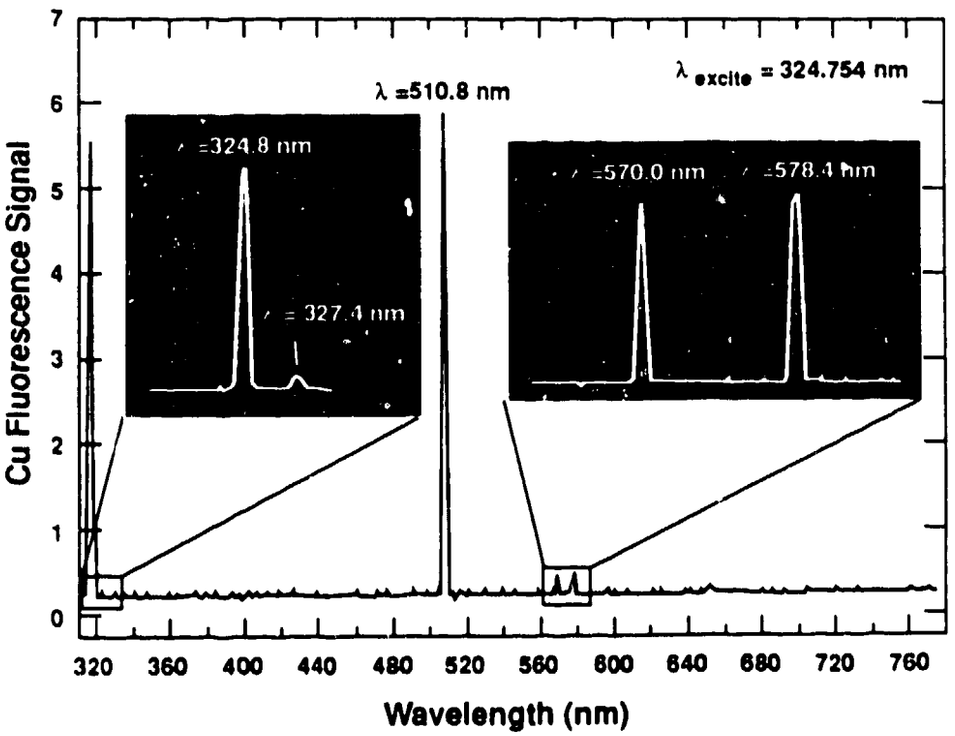

Fig. 3. Dispersed fluorescence scan of Cu atom exciting at 324.75 nm. The fact that we observe fluorescence at 327.4 nm and 578.4 nm indicates that energy transfer occurs quickly in the ^2P_J manifold. The spectrum was obtained under the same conditions as the excitation spectrum of Fig. 2.

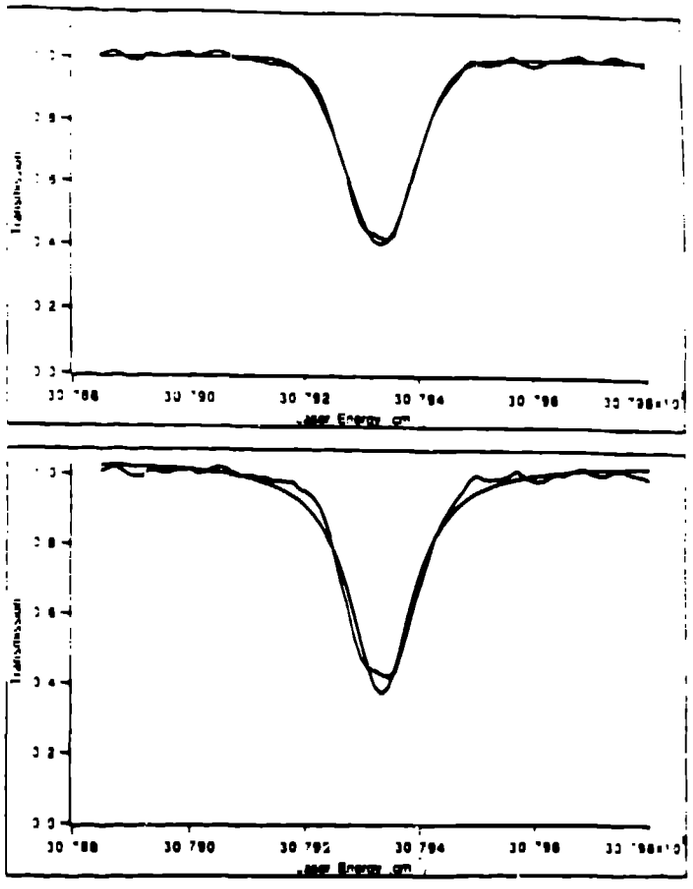

Fig. 4 Top panel: Gaussian fit to experimental absorption spectrum. The spectrum was obtained under the same conditions as the LIF spectrum of Fig. 2. The half-width of the fit is 1.43 cm^{-1}.
Bottom panel: Lorentzian fit to the same experimental absorption spectrum. Clearly the Gaussian fit is better indicating that Doppler broadening is the dominant broadening mechanism.

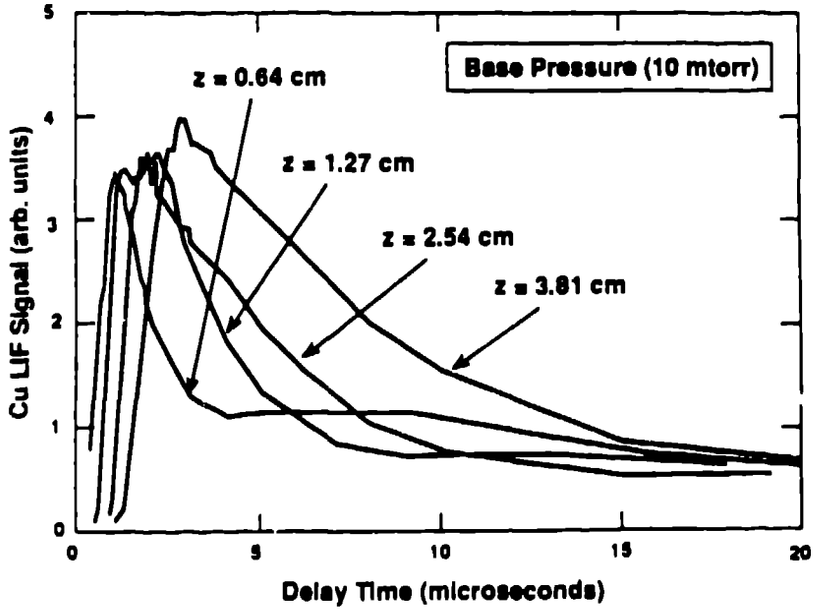

Fig. 5 Cu LIF time-of-flight curves obtained with 10 mtorr of He backing gas. The curves can be used to measure Cu velocity that is ~2 × 10^5 cm/s under these conditions.

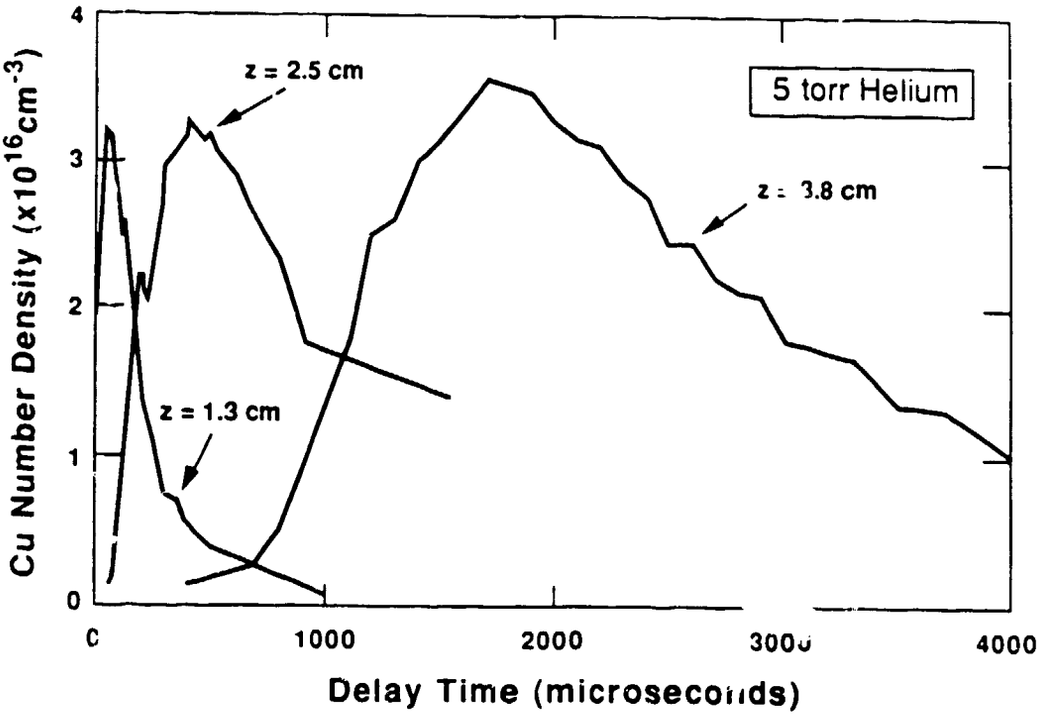

Fig. 6. Cu atom time-of-flight curves with 5 torr He backing gas. The He slows and broadens the time-of-flight curves when compared with those taken at low pressure (Fig. 5).

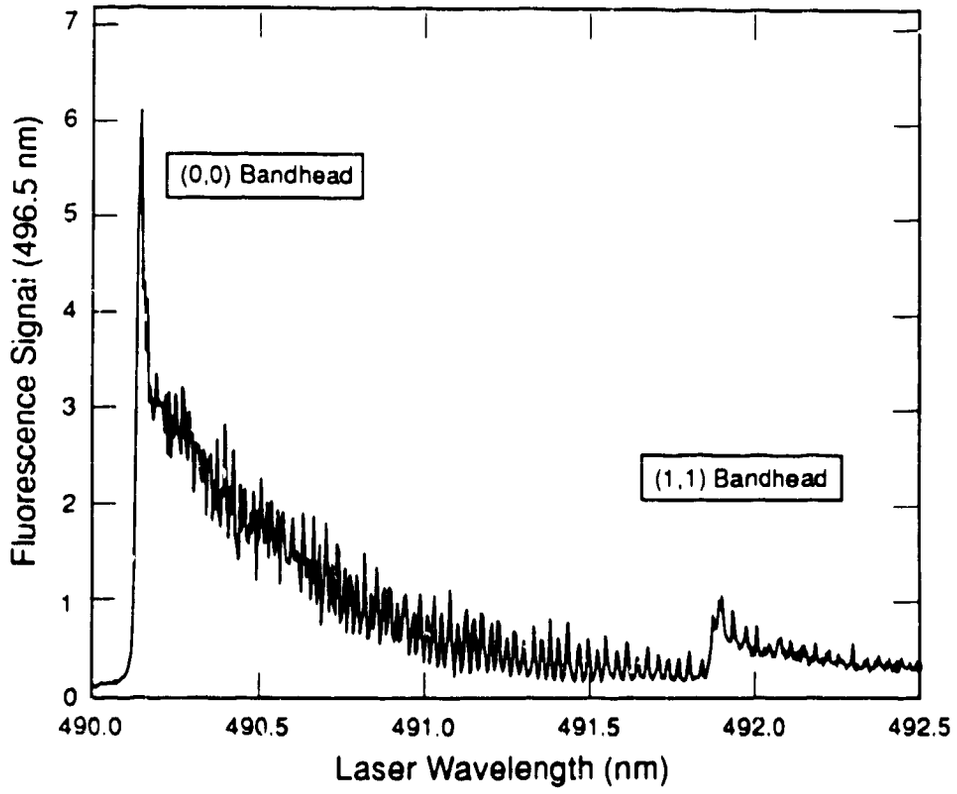

Fig. 7. LIF excitation scan of the Cu, A-X (0,0) band. Fluorescence is detected on the (0,1) band at 496.7 nm. The rotational structure can be simulated to obtain a temperature assuming a thermal distribution in the ground state. A vibrational temperature is obtained from the ratio of the (0,0) and (1,1) bandheads

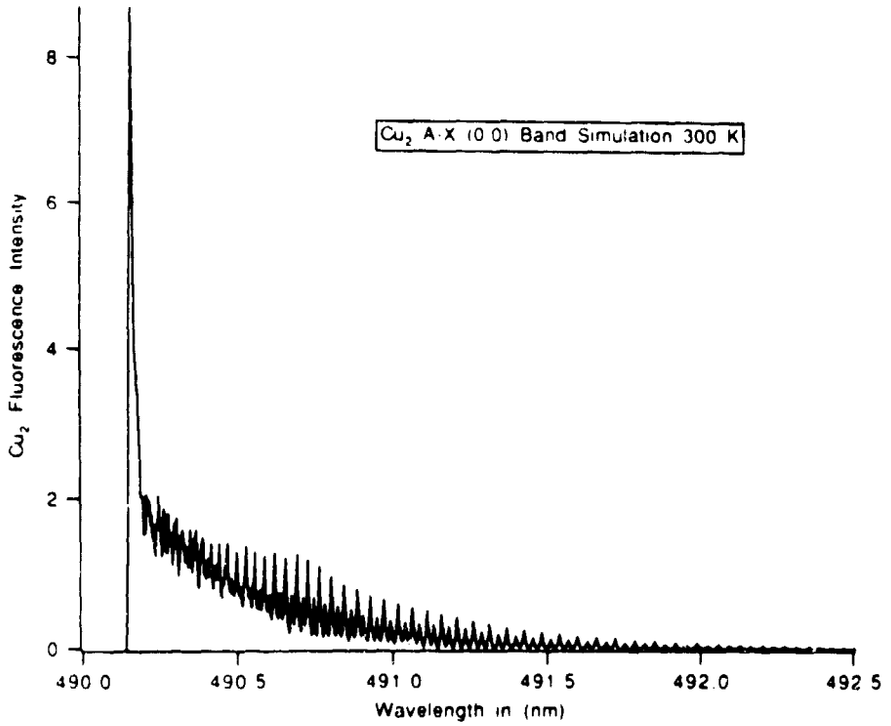

Fig. 8. Computer simulation of the Cu2 A-X (0,0) band at 300 K. The (1,1) band is not included in the simulation.

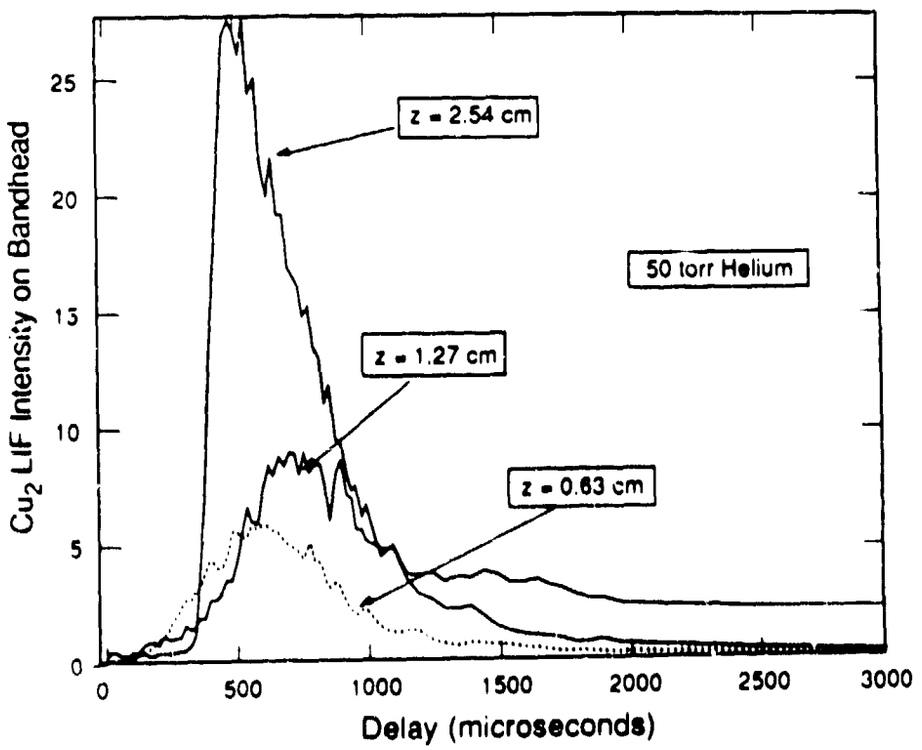

Fig. 9 Cu_2 LIF time-of-flight profiles obtained with 50-torr He backing gas. Notice that the curves indicate very slow movement of the Cu_2 and suggest that the Cu_2 is produced at relatively large distances from the target